Journal of Materials Chemistry A

Accepted Manuscript

ROYAL SOCIETY OF CHEMISTRY

www.rsc.org/materialsA

Cite this: DOI: 10.1039/c0xx00000x

www.rsc.org/xxxxxx

ARTICLE TYPE

Pt_2SnCu nanoalloy with surface enrichment of SnO_2 and Pt defects for high-efficient electrooxidation of ethanol

Meihua Huang,[a,b] Wangliang Wu,[a,b] Chuxin Wu,[a,b] and Lunhui Guan*[a,b]

Received (in XXX, XXX) Xth XXXXXXXXX 20XX, Accepted Xth XXXXXXXXX 20XX

DOI: 10.1039/b000000x

We artfully synthesized SnO_2 and Pt defects on the surface of carbon supported Pt_2SnCu nanoalloy (Pt_2SnCu-O-A/C) by in-situ surface oxidation and acid treatment. The Pt_2SnCu-O-A/C with surface enrichment of SnO_2 and Pt defects exhibits excellent electrocatalytic activities for the ethanol oxidation reaction (EOR) in comparison to the commercial Pt/C and PtRu/C. The surface activity and mass activity are 3.1 and 4.3 times greater than those of Pt/C. The enhanced activity for ethanol oxidation is attributed to the synergistic catalytic effect of SnO_2 and Pt defects.

Ethanol is one of the most hopeful fuels renewable energy applications due to its low toxicity, high availability from biomass production, and high energy density.[1,2] The direct ethanol fuel cell (DEFC) is fueled by the ethanol and provides electric energy, which offers distinct potential advantages over internal combustion engines. At present, Pt-based alloys or Pt-based composites as DEFC anode catalysts are considered to be the most important electrocatalysts. However, during the EOR, strongly adsorbed intermediates such as CO and CH_x poison the catalyst (e.g., Pt) surface and slow reaction kinetics considerably. Moreover, complete oxidation of ethanol into CO_2 via C-C bond cleavage is mechanistically difficult.[2] For the commercialization of DEFC, the sluggish kinetic of the EOR and incomplete oxidation of ethanol needs to be overcome.[1-3] Thus, the major challenge for the electrocatalysis of ethanol is to design catalysts, which should improve the kinetics of EOR and oxidize ethanol to CO_2 at low overpotentials.

A number of researchers have been motivated to develop high-efficient electrocatalysts for EOR.[4-8] Some latest studies have shown that Pt-Sn electrocatalysts are more active than PtRu/C electrocatalysts for ethanol electrooxidation.[2,9] In the EOR process, Sn can facilitate the formation of adsorbed OH species (OH_{ads}) via dissociative adsorption of water, which in turn helps the removal of adsorbed intermediates (CO_{ads}, $CH_{x,ads}$) on adjacent Pt sites (bifunctional effect). Sn also weakens the Pt-CO_{ads} bond by altering d-band properties of Pt orbitals (ligand effect).[2]

By adding noble metals such as Rh or Ir to Pt-Sn electrocatalysts, these catalysts also showed improved reaction kinetics and C-C splitting ability.[1,2,10,11] However, the scarcity and/or expense of Ir and Rh metals, even compared with Pt, impede their practical applications in DEFC. Therefore, improving C-C splitting of ethanol on the surface of Pt-Sn catalysts becomes imperative for DEFC.[2] Our group developed the Pt-Cu electrocatalyst which is effective in splitting the C-C bond in ethanol at room temperature, and the enhanced catalytic property of the Pt-Cu electrocatalyst is mainly attributed to the high density surface Pt defects (atomic steps and kinks with low coordination numbers on the surface of Pt-Cu alloy.[3] Du *et al.* found that the non-alloyed Pt_{46}-$(SnO_2)_{54}$ core-shell particles had a strong capability for C-C bond breaking of ethanol than pure Pt and intermetallic Pt/Sn, showing 4.1 times higher CO_2 peak partial pressure generated from EOR than the commercial Pt/C.[2] Magee *et al.* also prepared SnO_2 on polycrystalline Pt for ethanol electrooxidation and their studies suggested that the SnO_2 provided OH species for the effective oxidative removal of surface CO_{ads}.[12] Moreover, in situ infrared reflection absorption spectroscopy also suggested that the presence of OH species provided by the SnO_2 did not affect the C-C bond splitting ability of Pt active sites. However, the enhanced oxidation capabilities of small SnO_2 nanoparticles on Pt also leads to increased production partial oxidation products acetaldehyde and acetic acid, which lowers the overall selectivity and efficiency, because SnO_2 nanoparticles are randomly deposited on the polycrystalline Pt surface and not selectively deposited at the adjacent Pt defects. Hence, some Pt defects will clearly be blocked, which will decrease the effectiveness of C-C bond splitting.

Therefore, in this work, we hope that the SnO_2 oxides are at adjacent Pt defects through an artful and controlled synthesis method that avoids covering Pt defects and combines their merits of SnO_2 and Pt defects for the high-efficient EOR.

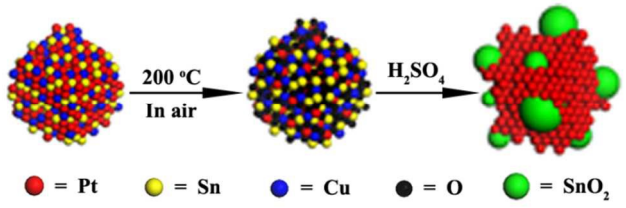

Fig. 1 Synthesis illustration of Pt_2SnCu-O-A/C

Fig. 1 shows the preparation process of the Pt_2SnCu nanoalloy with hybrid nanostructures (detailed synthesis procedures are presented in the experimental section). Firstly, the carbon supported Pt_2SnCu was prepared using the microwave-polyol technique.[3] When the carbon supported Pt_2SnCu nanoalloy were

heated at 200 °C, surface Sn and Cu atoms were oxidized, and exposed Sn and Cu atoms were further oxidized. So, the surface SnO_2 and CuO were formed by in-situ surface oxidation. Of course, some Cu_2O and SnO also existed on the surface layer. Then, near surface CuO, Cu_2O and SnO were dissolved in 0.5 M H_2SO_4 solution. The obtained sample is the carbon supported Pt_2SnCu nanoalloy with surface enrichment of SnO_2 and Pt defects. This structural design and synthetic method may preferably control the SnO_2 oxides at the adjacent Pt defects, which can make ample use of SnO_2 and adjacent Pt defects for the high-efficient EOR.

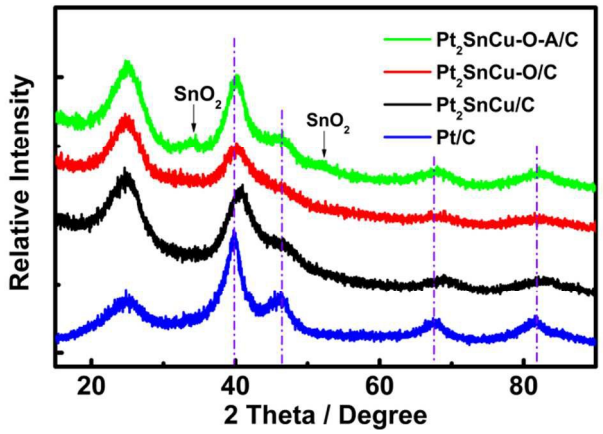

Fig. 2 XRD patterns of the synthesized samples and Pt/C.

The X-ray diffraction (XRD) patterns of the synthesized samples and Pt/C are shown in Fig. 2. The presence of the Vulcan XC-72R carbon resulted in broad reflections located around 25° in all patterns. Four diffraction peaks at about 2θ = 39.7°, 46.3°, 68.2° and 81.9° are characteristic of the face-centered cubic (FCC) structure of Pt. For Pt_2SnCu/C, Pt_2SnCu-O/C and Pt_2SnCu-O-A/C, it is observed a shift of the peaks relative to Pt (FCC) phase to higher angles compared to those of Pt/C, indicating a Pt-Sn-Cu alloy formation.[13,14] The Pt_2SnCu-O/C and Pt_2SnCu-O-A/C show a shift of the peaks relative to Pt (FCC) structure to lower angles compared to those of Pt_2SnCu/C, indicating structure changes of Pt_2SnCu/C. It may be that surface Sn and Cu atoms are oxidized, and exposed Sn and Cu atoms are further oxidized. Meanwhile, some Pt atoms are exposed on the surface of Pt_2SnCu/C. So the surface of Pt_2SnCu-O/C are composed of Sn oxides, Cu oxides and Pt shell, which result in the shift of the peaks relative to Pt (FCC) structure to lower angles compared to those of Pt_2SnCu/C. The peaks of Pt (FCC) phase in Pt_2SnCu-O/C might be the mixed peaks of Pt shell and Pt-Sn-Cu alloy core. The XRD patterns of Pt_2SnCu-O/C and Pt_2SnCu-O-A/C showed that the four diffraction peaks of Pt (FCC) structure were basically the same; however, the four peaks of Pt (FCC) structure of Pt_2SnCu-O-A/C become slightly stronger than those of Pt_2SnCu-O/C. Moreover, the peaks of SnO_2 are observed at about 2θ = 34.5° and 52.0°.[2] When the near surface CuO, Cu_2O and SnO are dissolved, the relative density of surface SnO_2 is increased and/or surface SnO_2 gathers. At the same time, exposed Pt atoms and original Pt atoms form Pt shell with Pt defects.[3] So, the peaks of SnO_2 in the Pt_2SnCu-O-A/C are detected and the peak intensity of Pt (FCC) structure of Pt_2SnCu-O-A/C become slightly stronger than that of Pt_2SnCu-O/C. The peaks of Pt (FCC) phase in the Pt_2SnCu-O-A/C might be the mixed peaks of Pt shell and Pt-Sn-Cu alloy core. Thus, the four diffraction peaks of Pt (FCC) structure in the Pt_2SnCu-O/C and Pt_2SnCu-O-A/C are basically the same. The XRD patterns of the PtSn/C and PtSn-O/C also demonstrate that in-situ surface oxidation is feasible to realize surface enrichment of SnO_2 and Pt defects. (See supporting information for more details).

Table 1. Samples composition measured by EDX and XPS.

Samples	Bulk composition (EDX) (Pt : Sn : Cu)	Surface composition (XPS) (Pt : Sn : Cu)
Pt_2SnCu/C	48 : 24 : 28	47 : 30 : 23
Pt_2SnCu-O/C	51 : 23 : 26	36 : 30 : 34
Pt_2SnCu-O-A/C	57 : 27 : 16	59 : 37 : 4

Table 2. Relative intensities of the Pt_2SnCu/C, Pt_2SnCu-O/C and Pt_2SnCu-O-A/C.

Valance state	Pt_2SnCu/C	Pt_2SnCu-O/C	Pt_2SnCu-O-A/C
Pt (0)	85.9 %	68.7 %	86.7 %
Pt (II + IV)	14.1 %	31.3 %	13.3 %
Cu (0)	26 %	19.2 %	100 %
Cu (I + II)	74 %	80.8 %	0 %

X-ray photoelectron spectroscopy (XPS) and Energy Dispersive X-Ray Spectroscopy (EDX) analyses of Pt_2SnCu/C, Pt_2SnCu-O/C and Pt_2SnCu-O-A/C were performed to compare the bulk and surface structures of the composites (Seeing Fig. S2-S4 for more details). The EDX and XPS results only taking into account of the metals are summarized in Table 1. It is found that the near surface elemental compositions of the Pt_2SnCu/C, Pt_2SnCu-O/C and Pt_2SnCu-O-A/C are not similar. Determination of near surface composition from the XPS results proves that the near surface of the Pt_2SnCu-O/C is enriched in Sn and Cu, as compared to that of Pt_2SnCu/C. Then, the near surface of the Pt_2SnCu-O-A/C is rare in Cu as compared to that of the Pt_2SnCu/C and Pt_2SnCu-O/C. It can be noted that most of the XPS studies reported in the literature data do not allow definition between Sn (II), Sn (IV) and Sn^0 species because of a small difference in the binding energy for Sn (II) and Sn (IV) species and chemisorbed oxygen in Sn^0.[13,14] So we were not able to fit the overall Sn 3d spectrum of Pt_2SnCu/C precisely including the Sn (II), Sn (IV) and Sn (0) peaks. In line with the experimental treatment and the results of XRD and XPS, the surface presence of Sn^0 (alloyed) species in the Pt_2SnCu-O/C and Pt_2SnCu-O-A/C should be discarded. The XPS results with corresponding relative intensities of valance state are presented in Table 2. In the near surface elemental compositions of Pt_2SnCu-O/C, the ratios of Pt and Cu oxidation state are higher than those of Pt_2SnCu/C, because the Pt_2SnCu-O/C is prepared through the in-situ surface oxidation of Pt_2SnCu/C. However, in the near surface elemental compositions of Pt_2SnCu-O-A/C, the ratios of Pt and Cu oxidation state are lower than those of Pt_2SnCu-O/C, because the

near surface CuO, Cu_2O and SnO of Pt_2SnCu-O/C are dissolved and Pt^0 atoms are exposed. So, the results show that, by the in-situ surface oxidation, surface Sn and Cu are oxidized, and exposed Sn and Cu are further oxidized. Meanwhile, some surface Pt atoms and exposed Pt atoms perhaps absorb oxygen atoms or are oxidized. When the Pt_2SnCu-O/C was immersed in 0.5 M H_2SO_4 solution, the near surface CuO, Cu_2O and SnO of Pt_2SnCu-O-A/C were dissolved. Hence, surface SnO_2 is retained and gathered on the surface of Pt_2SnCu-O-A/C and more Pt^0 atoms are exposed on the surface of Pt_2SnCu-O-A/C.

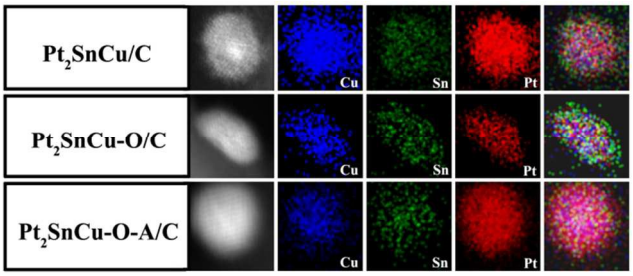

Fig. 3 STEM images and elemental scanning images of Pt_2SnCu/C, Pt_2SnCu-O/C and Pt_2SnCu-O-A/C.

In order to understand the surface structure changes of Pt_2SnCu/C, Pt_2SnCu-O/C and Pt_2SnCu-O-A/C, we also used high resolution transmission electron microscopy (HRTEM) and scanning transmission electron microscopy energy-dispersive X-ray spectroscopy (STEM-EDS) to map the distribution of Pt, Sn and Cu. The nanoparticles of Pt_2SnCu/C, Pt_2SnCu-O/C and Pt_2SnCu-O-A/C have better dispersion. The average particle size for Pt_2SnCu/C, Pt_2SnCu-O/C and Pt_2SnCu-O-A/C are 2.2, 2.7 and 2.7 nm, respectively, as can be seen in the TEM images (Fig. S5-S7).The Pt, Sn and Cu EDS maps of Pt_2SnCu/C show a homogeneous distribution of the three elements over the entire particle (Fig. 3). However, the EDS maps of Pt_2SnCu-O/C reveal that a Sn and Cu-rich shell is formed around the Pt-Sn-Cu alloy core of the Pt_2SnCu-O/C. Then, the EDS maps of Pt_2SnCu-O-A/C (Fig. 3 and Fig. S8) reveal that a Sn and Pt-rich shell is formed around the Pt-Sn-Cu core of the Pt_2SnCu-O-A/C. Moreover, the Sn elements are distributed over the Pt elements. On the basis of STEM-EDS data, we may basically deduce that when the Pt_2SnCu/C was heated at 200 ^oC in air, the surface Cu and Sn atoms were oxidized and exposed Cu and Sn atoms were further oxidized. Of course, some surface Pt atoms and exposed Pt atoms were also oxidized or absorb oxygen atoms. In this process, surface Cu and Sn oxides are rich on the surface of Pt_2SnCu-O/C. When the Pt_2SnCu-O/C was immersed in 0.5 M H_2SO_4 solution, surface Cu oxides and SnO were dissolved and SnO_2 was retained and gathered on the surface of Pt_2SnCu-O-A/C. Meanwhile, exposed Pt atoms and original Pt atoms formed Pt shell.

Based on aboved characterizations and our previous report, our experimental design and synthesis are feasible.[3] The Pt_2SnCu-O-A/C is surface enrichment of SnO_2 and Pt defects with Pt-Sn-Cu alloy core. Maybe, the Pt_2SnCu-O-A/C with hybrid nanostructures can exhibit synergistically enhanced ethanol oxidation properties. The electrochemically active surface areas (ECASAs) of the PtSn/C, Pt_2Sn-O/C, Pt_2SnCu-O-A/C, and Pt/C were measured using cyclic voltammograms (CVs) in 0.5 M H_2SO_4 (Fig. 4a). Their ECASAs of the PtSn/C, PtSn-O/C, Pt_2SnCu-O-A/C, and Pt/C are 62.0, 57.1, 98.4 and 71.5 $m^2\ g^{-1}$, respectively. Due to in-situ surface oxidation, the surface of some Pt atoms is covered by Sn oxides. So, the ECASA of PtSn-O/C is lower than that of the PtSn/C. However, the ECASA of Pt_2SnCu-O-A/C is larger than those of the PtSn/C and PtSn-O/C, because the surface Cu oxides and SnO were dissolved and more Pt^0 atoms are exposed on the surface of Pt_2SnCu-O-A/C. At the same time, Pt-based alloy makes that more Pt atoms are used, which is consistent with the previous report.[15] The results further proved that our experimental design and synthesis are feasible. And the Pt_2SnCu-O-A/C has the desirable structure.

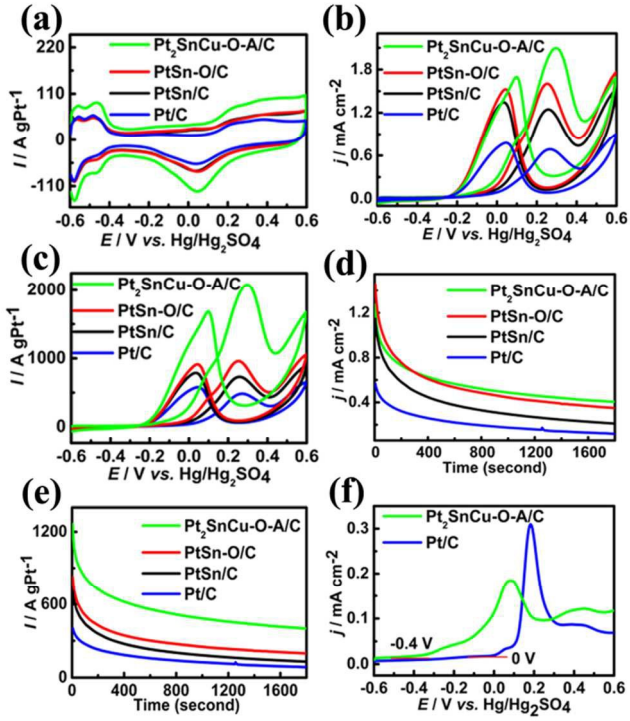

Fig. 4 (a) CVs on different catalysts at 50 mV s^{-1}. (b) and (c) Specific activity and mass activity of different catalysts at 50 mV s^{-1}. (d) and (e) Current-time curves of different catalysts at 0.2 V. (f) CO stripping voltammograms of different catalysts at 50 mV s^{-1}.

Fig. 4b-c depict the CVs of the PtSn/C, PtSn-O/C, Pt_2SnCu-O-A/C and Pt/C for ethanol oxidation. The oxidation current was normalized to the electroactive Pt surface area and Pt loading mass, respectively. As shown in Fig. 4b-c, the order of onset potentials is Pt_2SnCu-O-A/C < Pt_2Sn-O/C < PtSn/C < Pt/C. The forward peak current density measured for the Pt_2SnCu-O-A/C is 2.1 mA cm^{-2}, 3.1 times greater than that of Pt/C. The result is better than that of previous reports.[1,2] The peak mass activity of the Pt_2SnCu-O-A/C is 2078.1 A g^{-1}, 4.3 times greater than that of Pt/C. The result is also superior to previous reports of Pt-based catalysts.[4,14,16-19] In the forward scan the electrooxidation of ethanol shows one anodic peak while in some reports has shown two anodic peaks. The reason is due to the different scan range.[20] Long-term chronoamperometric experiments were conducted to evaluate the electrocatalytic activity and stability of the catalysts

under continuous operating conditions. Fig. 4d-e show the current-versus-time curves recorded at 0.2 V for 1800 sec in 1.0 M CH_3CH_2OH + 0.5 M H_2SO_4. The results clearly demonstrate that the presence of surface SnO_2 and Pt defects in Pt_2SnCu-O-A/C endows the Pt_2SnCu-O-A/C with outstanding electrocatalytic activity. For clarity, the Pt_2Sn-O/C and PtSn/C are not further studied.

A key limiting factor for DEFCs catalysts is the intermediate species (i.e., CO) generated during the EOR. Such intermediates can strongly adsorb onto the surface of Pt atoms, resulting in low-power densities.[5,21] Thus, CO oxidation was investigated to examine intermediate oxidation on the Pt_2SnCu-O-A/C and Pt/C. The results are presented in Fig. 6f. The onset potentials of Pt_2SnCu-O-A/C and Pt/C for CO oxidation are -400 and 0 mV, respectively. Consequently, the Pt_2SnCu-O-A/C is less susceptible to self-poisoning compared with Pt/C. The anti-poisoning activity of the Pt_2SnCu-O-A/C is superior to our previous report.[3]

Commercial PtRu/C is also investigated to examine ethanol and CO oxidation. The tests showed that the Pt_2SnCu-O-A/C also exhibited enhanced electrocatalytic activity for ethanol and CO oxidation compared with PtRu/C (Seeing Fig. S9 for more details).

Conclusions

In summary, the Pt_2SnCu-O-A/C was synthesized by the in-situ surface oxidation following acid-treatment. Detailed investigation of the structure revealed that the Pt_2SnCu-O-A/C has a surface enrichment of SnO_2 and Pt defects with a Pt-Sn-Cu alloy core. Electrochemical tests for EOR demonstrated that the Pt_2SnCu-O-A/C has a superior surface and mass activity compared with Pt/C and PtRu/C. This outstanding performance toward ethanol oxidation might be attributed to the synergistic effect of surface SnO_2 and Pt defects. The present study provides a facile and efficient synthetic technique to prepare Pt-based catalysts with hybrid nanostructures for high-efficient EOR, which would promote the development of Pt-based anode catalysts in DEFCs.

Acknowledgments

This research was supported by the Natural Science Foundation of Fujian Province (grant no. 2014J01064 and 2013J06006), the National Natural Science Foundation of China (Grant no. 91127020, 21171163 and 21101154) and the National Key Project on Basic Research (grant no. 2011CB935904). The authors appreciate Professor Chuanhong Jin and Doctor Hongtao Wang at Department of Materials Science and Engineering, Zhejiang University, for STEM-EDS characterization.

Notes and references

[a] *Key Laboratory of Design and Assembly of Functional Nanostructures, Fujian Institute of Research on the Structure of Matter, Chinese Academy of Sciences, Fuzhou, 350002, China.*

[b] *Fujian Provincial Key Laboratory of Nanomaterials, Fujian Institute of Research on the Structure of Matter, Chinese Academy of Sciences, Fuzhou, 350002, China.*
E-mail: guanlh@fjirsm.ac.cn.

† Electronic Supplementary Information (ESI) available: [details of any supplementary information available should be included here]. See DOI: 10.1039/b000000x/

1 M. Li, D. A. Cullen, K. Sasaki, N. S. Marinkovic, K. More and R. R. Adzic, *J. Am. Chem. Soc.*, 2013, **135**, 132.
2 W. X. Du, G. X. Yang, E. Wong, N. A. Deskins, A. I. Frenkel, D. Su and X. W. Teng, *J. Am. Chem. Soc.*, 2014, **136**, 10862.
3 M. H. Huang, Y. Y. Jiang, C. H. Jin, J. Ren, Z. Y. Zhou and L. H. Guan, *Electrochimi. Acta*, 2014, **125**, 29.
4 F. Saleem, Z. C. Zhang, B. Xu, X. B. Xu, P. L. He and X. Wang, *J. Am. Chem. Soc.*, 2013, **135**, 18304
5 M. Carmo, R. C. Sekol, S. Y. Ding, G. Kumar, J. Schroers and A. D. Taylor, *ACS Nano*, 2011, **5**, 2979.
6 W. X. Du, Q. Wang, D. Saxner, N. A. Deskins, D. Su, J. E. Krzanowski, A. I. Frenkel and X. W. Teng, *J. Am. Chem. Soc.*, 2011, **133**, 15172.
7 M. H. Huang, G. F. Dong, N. Wang, J. X. Xu and L. H. Guan, *Energy Environ. Sci.*, 2011, **4**, 4513.
8 Z. Y. Zhou, Z. Z. Huang, D. J. Chen, Q. Wang, N. Tian and S. G. Sun, *Angew. Chem. Int. Ed.*, 2010, **49**, 411.
9 M. Nakamura, R. Imai, N. Otsuka, N. Hoshi, O. Sakata, *J. Phys. Chem. C*, 2013, **117**, 18139.
10 A. Kowal, M. Li, M. Shao, K. Sasaki, M. B. Vukmirovic, J. Zhang, N. S. Marinkovic, P. Liu, A. I. Frenkel and R. R. Adzic, *Nat. Mater.*, 2009, **8**, 325.
11 M. Li, A. Kowal, K. Sasaki, N. Marinkovic, D. Su, E. Korach, P. Liu and R. R. Adzic, *Electrochim. Acta*, 2010, **55**, 4331.
12 J. W. Magee, W. P. Zhou and M. G. White, *Appl. Catal. B: Environ.*, 2014, **152-153**, 397.
13 E. Lee, A. Murthy and A. Manthiram, *Electrochimi. Acta*, 2011, **56**, 1611.
14 S. Beyhana, J. M. Léger and F. Kadırgan, *Appl. Catal. B: Environ.*, 2013, **130-131**, 305.
15 F. H. Li, Y. Q. Guo, M. X.Chen, H. X. Qiu, X. Y. Sun, W. Wang, Y. Liu, J. P. Gao, *Int. J. Hydrogen Energy*, 2013, **38**, 14242.
16 Z. Q. Yao, M. S. Zhu, F. X. Jiang, Y. K. Du, C. Y. Wang and P. Yang, *J. Mater. Chem.*, 2012, **22**, 13707.
17 D. González-Quijano, W. J. Pech-Rodríguez, J. I. Escalante-García, G. Vargas-Gutiérrez, F. J. Rodríguez-Varela, *Int. J. Hydrogen Energy*, 2014, **39**, 16676.
18 Y. Wang, G. C. Wu, Y. Z. Wang, X. M. Wang, *Electrochimi. Acta*, 2014, **130**, 135.
19 C. C. Kung, P. Y. Lin, Y. H. Xue, R. Akolkar, L. M. Dai, X. Yu, C. C. Liu, *J. Power Sources*, 2014, **256**, 329.
20 B. Habibi, E. Dadashpour, *Int. J. Hydrogen Energy*, 2013, **38**, 5425.
21 E. Reddington, A. Sapienza and B. Gurau, R. Viswanathan, S. Sarangapani, E. S. Smotkin and T. E. Mallouk, *Science*, 1998, **280**, 1735.

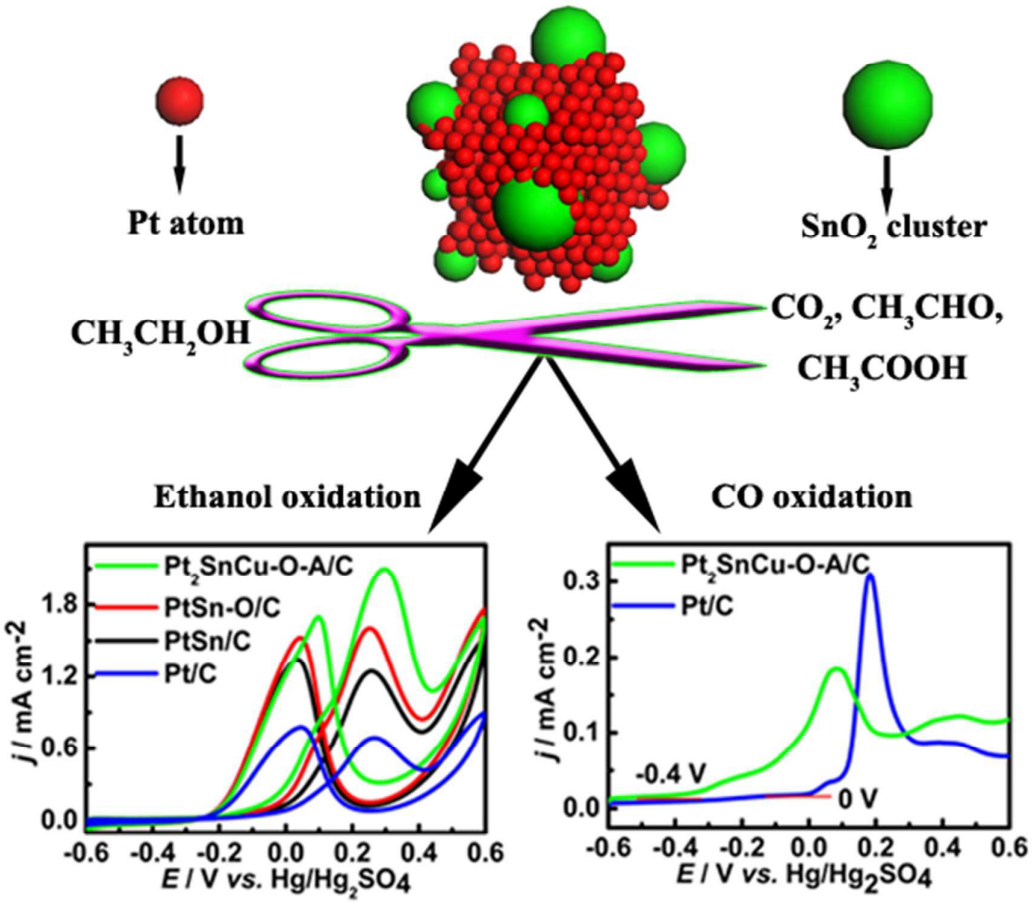

The Pt_2SnCu-O-A/C with surface enrichment of SnO_2 and Pt defects exhibits excellent electrocatalytic activities for the ethanol oxidation in comparison to the commercial Pt/C and PtRu/C. The synthesis method may provide new opportunities to design and fabricate hybrid nanostructures with interesting physicochemical properties.